JOURNAL OF APPLIED ELECTROCHEMISTRY 24 (1994) 396–403

Electrochemical reduction of silver thiosulphate complexes
Part II Mechanism and kinetics

A. HUBIN, J. VEREECKEN

Vrije Universiteit Brussel, Department of Metallurgy, Electrochemistry and Materials Science, Pleinlaan 2, B-1050 Brussels, Belgium

Received 19 October 1992; revised 8 July 1993

In this paper the thermodynamic data for complex formation between Ag^+ and $S_2O_3^{2-}$ ions, determined previously, are applied to kinetic investigation of the reduction of silver thiosulphate complexes. Both electrochemical (linear sweep voltammetry on a rotating disc electrode) and surface analytical (Auger electron spectroscopy) techniques are used. The deposits resulting from the electrodeposition of silver thiosulphate complexes are shown to be composed of silver and to be polycrystalline. The reduction follows a mechanism involving mass and charge transfer and chemical reaction steps. The relevant kinetic parameters are calculated and a rate equation describing the kinetics of the reduction is given.

List of symbols

a activity (M)
c concentration (M)
j current density ($A\,m^{-2}$)
j_c current density of charge transfer ($A\,m^{-2}$)
j_m current density of mass transfer ($A\,m^{-2}$)
k rate constant ($m\,s^{-1}$)
y activity coefficient (molarity scale)

D diffusion coefficient against gradient of concentration ($m^2\,s^{-1}$)
$\boldsymbol{D}$ diffusion coefficient against gradient of electrochemical potential ($m^2\,s^{-1}$)
E electrode potential vs NHE (V)
I ionic strength (M)
T temperature (K)

Greek symbols

α transfer coefficient
β_{ln} stability constant of $Ag(S_2O_3)_n^{(2n-1)-}$
ν kinematic viscosity ($m^2\,s^{-1}$)
ω rotation speed of the electrode ($rad\,s^{-1}$)

Indices

b bulk of the solution
f free (= uncomplexed)
l,n related to complex $Ag(S_2O_3)_n^{(2n-1)-}$
t total

Constants

F Faraday constant (96 486 $A\,s\,mol^{-1}$)
R universal gas constant (8.3145 $J\,mol^{-1}\,K^{-1}$)

1. Introduction

For applications in photography and electroplating [1] the kinetics of the electrodeposition of silver thiosulphate complexes, together with the characteristics of the composition of the resulting deposits, are of major importance. The aim of the present work is the study of the kinetics of the reduction of silver thiosulphate complexes and the determination of the chemical composition of the silver deposit by means of surface analytical techniques. The thermodynamics of complex formation between Ag^+ and $S_2O_3^{2-}$ have already been treated [1].

2. Experimental details

2.1. *Electrochemical techniques*

Solution preparation and calculation of the concentration parameters were as discussed in [1]. Measurements were carried out on a rotating silver (99.99% Johnson, Matthey) disc electrode with a radius of 2 mm. A platinum (Johnson, Matthey) counter electrode with large area and a calomel electrode with saturated KCl solution (Tacussel) were used. It was possible to work under thermostatic conditions (25.0 ± 0.1 °C) by using a double walled electrolytic cell. Before each experiment, the electrode was polished with diamond spray

0021-891X 1994 Chapman & Hall

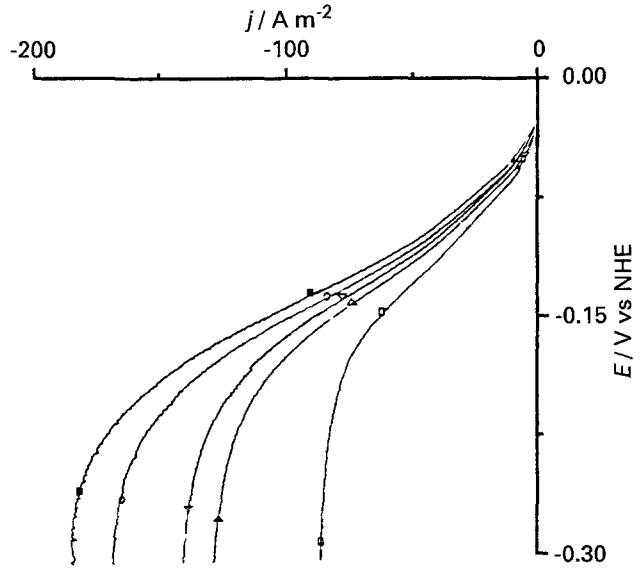

Fig. 1. Voltammograms as a function of electrode rotation speed, ω: 344 (□), 773 (△), 954 (▽), 1375 (○), 1614 (■) r.p.m. $(c_{Ag^+})_t = 0.04\,mol\,dm^{-3}$; scan rate = $1\,mV\,s^{-1}$; ohmic drop corrected.

(Buehler Metadi compound 5 and 1 μm) and rinsed ultrasonically in twice demineralized water and chloroform (p.a. Merck).

Linear sweep voltammetry was performed at a scan rate of $1\,mV\,s^{-1}$ using a potentiostat with built-in generator (Princeton Applied Research, PAR model 273). Voltammograms were digitally recorded with an oscilloscope (Nicolet, model 210) and transferred to and analysed by an Apple Macintosh computer.

The electrolyte resistance was deduced from high frequency (65 kHz to 100 Hz) impedance measurements under potentiostatic control (signal amplitude 10 mV). Details of the measurement and data treatment are found in [2].

Viscosity measurements were done with a Haake microviscositymeter.

2.2. *Surface analytical techniques*

The characterization of silver deposits, resulting from the electrochemical reduction of thiosulphate complexes at constant potential, was carried out using three techniques: Auger electron spectroscopy (AES) (PHI 545 with cylindrical mirror analyser), scanning electron microscopy (SEM) (Jeol JSM 50-A) and reflection electron diffraction (Seifert).

For the AES measurements, standard samples from the following powders were prepared by pressing them into indium foil (Johnson, Matthey): Ag_2S (p.a. Johnson, Matthey), Ag_2O (purum p.a. Fluka AG), K_2SO_4 (purum Fluka AG), Ag_2SO_4 and $Na_2S_2O_3$ (p.a. UCB). As pure silver standards, polycrystalline silver (99.99% Johnson, Matthey) and silver (99.99% Balzers), evaporated onto glass, were used.

Spectra, both on silver deposits and standards, were recorded in the E[dN(E)/dE] derivative mode under constant conditions: defocused 0.5 mA and 1000 eV primary electron beam, 3 V peak-to-peak modulation voltage and 0.1 s time constant. For depth profiling of the silver deposits, gold, instead of silver, electrodes were used. Profiling conditions were: 5×10^{-5} torr argon pressure, 10 mA and 2000 eV primary ion beam and 100 s sputtering time.

3. Results and discussion

3.1. *Electrochemical analysis*

Voltammograms are recorded as a function of electrode rotation speed (Fig. 1) and solution concentration (Fig. 2).

At low overpotentials, the current density increases strongly with potential, whereas it becomes almost independent of potential, but a function of electrode rotation speed at high overpotentials. In an intermediate zone, the current density depends both on potential and rotation speed. At increasing total silver concentration the value of the overpotential, at which the influence of the potential on the current density falls, increases.

These results strongly suggest the competing effects of electron transfer and mass transfer rates so that the current density must comply with Equation 1. This is the steady state convective diffusion equation,

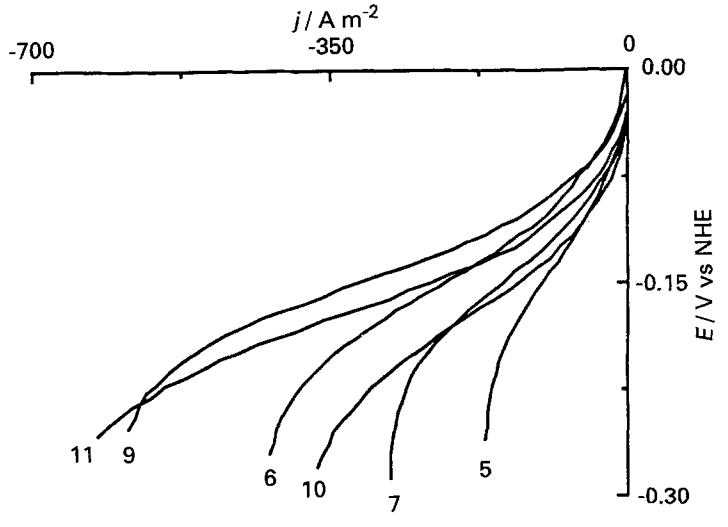

Fig. 2. Voltammograms as a function of solution concentration. Scan rate: $1\,mV\,s^{-1}$; rotation speed: 1375 r.p.m.; ohmic drop corrected. Numbers on the plot refer to solution numbers in [1].

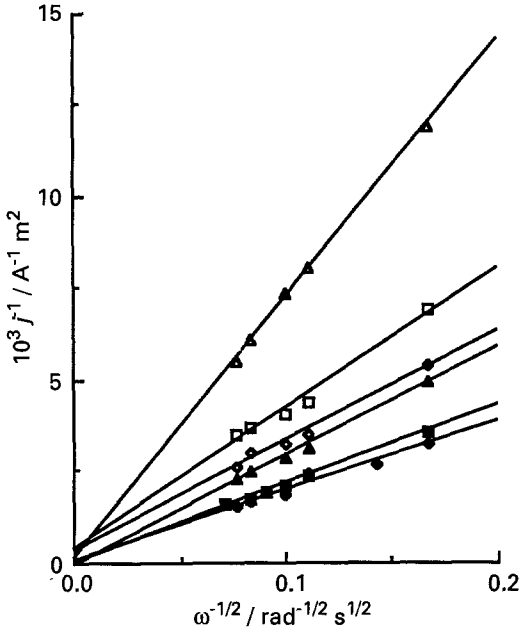

Fig. 3. Inverse of current density, j^{-1}, against inverse of square root of rotation speed, $\omega^{-1/2}$, plot. Solution number [1]: (△) 5, (□) 7, (◇) 10, (▲) 6, (■) 9, (◆) 11; $E = -0.250$ V vs NHE.

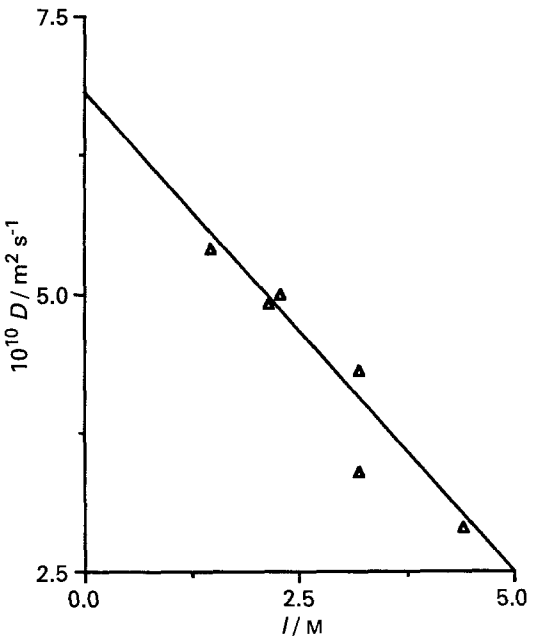

Fig. 5. Global diffusion coefficient, D, as a function of ionic strength, I.

neglecting migration effects, for a uniformly accessible rotating disc electrode and a first order reduction reaction [3, 4]:

$$1/j = 1/j_c + 1/j_m \tag{1}$$

with

$$j_c = -Fk \exp\left(\frac{-\alpha FE}{RT}\right) a_b \tag{1a}$$

$$j_m = -0.62 F \nu^{-1/6} D^{2/3} \omega^{1/2} c_b \tag{1b}$$

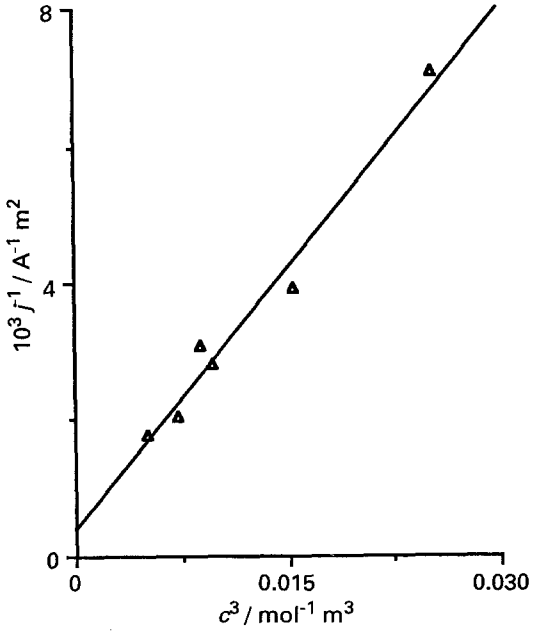

Fig. 4. Inverse in current density, j^{-1}, against inverse of total silver concentration, c^{-1}, plot. Rotation speed = 950 r.p.m., $E = -0.250$ V vs NHE.

j^{-1} is plotted against $\omega^{-1/2}$ in Fig. 3 and against $(c_{Ag})_t^{-1}$ in Fig. 4.

j^{-1} being a linear function of both parameters, a model involving mass and charge transfer steps is proposed corresponding to a rate equation of type (1). The mass and charge transfer parameters are determined in the following.

3.1.1. Determination of mass transfer parameters. Assuming that all silver components are diffusing in the solution with equal diffusion coefficients, c_b is equal to $(c_{Ag})_t$. D is calculated from the slopes of the straight lines of Fig. 3 (measured values of the kinematic viscosities are found in Table 1), and plotted as a function of the ionic strength of the solution in Fig. 5. The values are scattered round a straight line. The same applies for the points in the j^{-1} against c^{-1} plot of Fig. 4.

Since the amount of silver present as $Ag(S_2O_3)_3^{5-}$ is different in the solutions [1], this suggests that $Ag(S_2O_3)_2^{3-}$ and $Ag(S_2O_3)_3^{5-}$ have different diffusion coefficients, hereinafter called $D_{1,2}$ and $D_{1,3}$.

To determine $D_{1,2}$ and $D_{1,3}$ as a function of ionic strength, measurements were performed in solutions of varying concentrations. Parameters were: amount

Table 1. Measured values of the kinematic viscosity

$10^6 \nu$ /m^2 s^{-1}	*Solution numbers**
0.90	1, 1.1, 2, 2.1, 3, 3.1, 4, 4.1, 12, 13
1.00	6
1.05	7, 8, 9, 14
1.10	5, 10, 11
1.15	15

* Solution numbers as in [1].

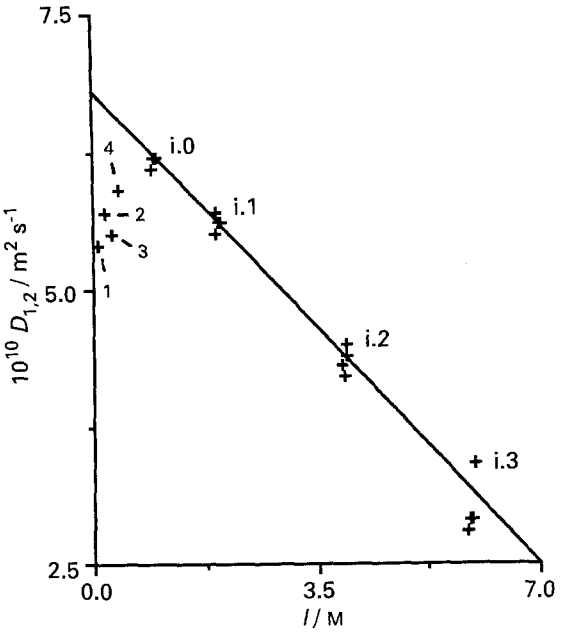

Fig. 6. Diffusion coefficient of $Ag(S_2O_3)_2^{3-}$, $D_{1,2}$ as a function of ionic strength, I. Numbers on the plot refer to solution numbers in [1]; $i = 1$ to 4.

of $Ag(S_2O_3)_3^{5-}$ (from 0 to 58%) and ionic strength (adjusted by means of $NaNO_3$). A detailed table of concentration parameters is found in [1].

First $D_{1,2}$ was evaluated from measurements in solutions without $Ag(S_2O_3)_3^{5-}$. Then, $D_{1,3}$ was determined in solutions containing both complexes. The equations used were:

$$D_{1,2} = \left[\frac{1}{sF\,0.62\nu^{-1/6}c_{1,2}}\right]^{3/2} \qquad (2)$$

$$D_{1,3} = \left[\frac{1}{sF\,0.62\nu^{-1/6}c_{1,3}} - \frac{c_{1,2}}{c_{1,3}}D_{1,2}^{2/3}\right]^{3/2} \qquad (3)$$

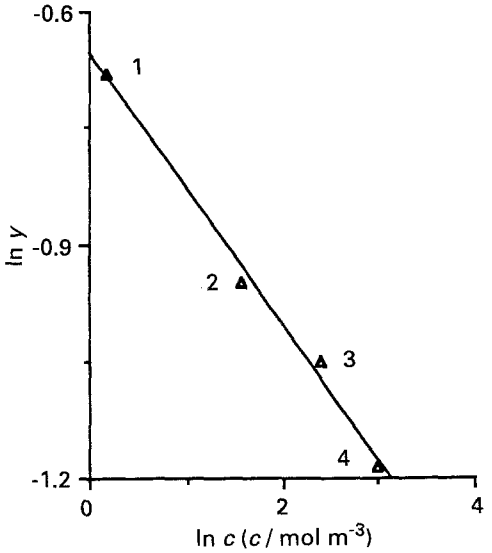

Fig. 7. Variation of the activity coefficient of $Ag(S_2O_3)_2^{3-}$, y, as a function of its concentration, c (bi-logarithmic diagram). Numbers on the plot refer to solution numbers in [1].

Table 2. Comparison of different values of the diffusion coefficient of $Ag(S_2O_3)_2^{3-}$

*Solution number**	$10^{10}\ D_{1,2}$† *calculated* /m^2 s^{-1}	$10^{10}\ D_{1,2}$‡ *experimental* /m^2 s^{-1}	$10^{10}\ \boldsymbol{D}_{1,2}$§ *experimental* /m^2 s^{-1}
1	6.7	5.4	6.5
2	6.7	5.7	6.9
3	6.6	5.5	6.7
4	6.5	5.9	7.2

† $D_{1,2}$ calculated = according to Equation 4
‡ $D_{1,2}$ experimental = measured value
§ $\boldsymbol{D}_{1,2}$ experimental = corrected value of $D_{1,2}$
* Solution numbers as in [1].

s is the slope of the straight line of the j^{-1} against $\omega^{-1/2}$ plot.

Figure 6 shows $D_{1,2}$ as a function of ionic strength. $D_{1,2}$ decreases linearly with ionic strength, except for solutions with no added supporting electrolyte. Linear regression, excluding the values of $D_{1,2}$ for solutions 1 to 4, gives

$$D_{1,2}(I) = 6.8 \times 10^{-10} - 6.4 \times 10^{-11} I \qquad (4)$$

Table 2 compares, for solutions 1 to 4, the experimental values of $D_{1,2}$ with those calculated from the regression Equation 4.

Using Equation 2 for the calculation of a diffusion coefficient implies that the activity coefficient of the diffusing species is independent of its concentration [5]. As shown in [1], this is the case for solutions containing supporting electrolyte (*i*.0 to *i*.3 with $i = 1, 2, 3$ or 4), but not for the solutions 1 to 4 without supporting electrolyte. Consequently, D and $\boldsymbol{D}$, respectively with gradient of concentration and gradient of electrochemical potential as driving force, must be distinguished. The first is the measured

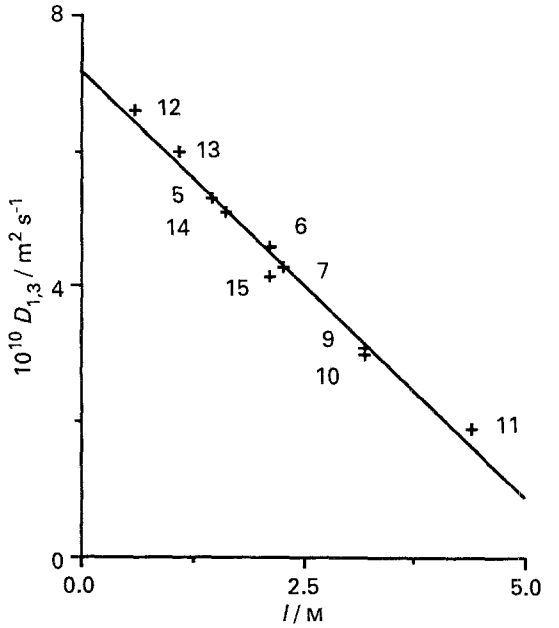

Fig. 8. Diffusion coefficient of $Ag(S_2O_3)_3^{5-}$, $D_{1,3}$, as a function of ionic strength, I. Numbers on the plot refer to solution numbers in [1].

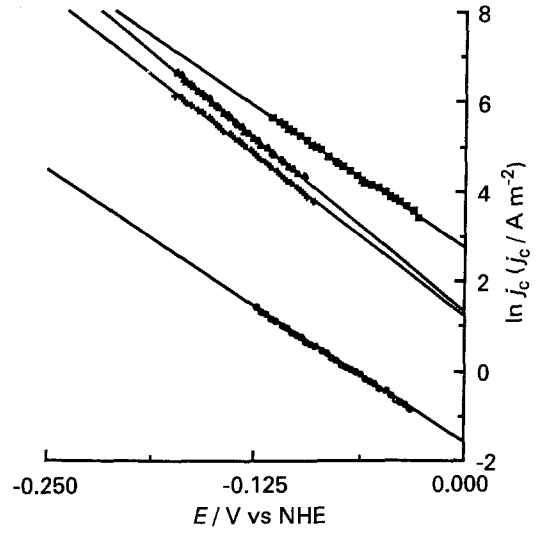

Fig. 9. Variation of current density of charge transfer, j_c, as a function of electrode potential, E (logarithmic diagram). Solution number [1]: (■) 4.1, (▲) 11, (+) 5, (○) 1.

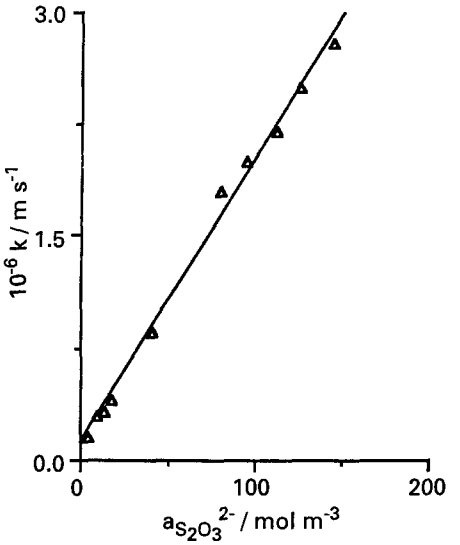

Fig. 10. Rate constant, k, as a function of the activity of $S_2O_3^{2-}$, $a_{S_2O_3^{2-}}$.

diffusion coefficient; the latter is independent of concentration [5]. Neglecting the interaction between $Na_3Ag(S_2O_3)_2$ and the other electrolytes and taking the total concentration equal to the solvent concentration, D and $\boldsymbol{D}$ are correlated by Equation 5 [6]:

$$D_{1,2} = \boldsymbol{D}_{1,2}\left(1 + \frac{\mathrm{d}\ln y_{1,2}}{\mathrm{d}\ln c_{1,2}}\right) \qquad (5)$$

Figure 7 shows the $\ln y_{1,2}$ against $\ln c_{1,2}$ plot. With linear regression, a value of -0.17 for $\mathrm{d}\ln y_{1,2}/\mathrm{d}\ln c_{1,2}$ is determined, and the value of the concentration independent diffusion coefficient is 1.2 times greater than the experimental value. As can be seen in Table 2, the corrected $D_{1,2}$ values fit Equation 4, except for solution 4. Due to its intermediate ionic strength, the activity coefficient shows a transient behaviour between linear dependence and independence of concentration.

Figure 8 gives $D_{1,3}$ calculated from Equations 3 and 4, as a function of ionic strength. Like $D_{1,2}$, $D_{1,3}$ is a linearly decreasing function of I, and the regression equation is

$$D_{1,3} = 7.2 \times 10^{-10} - 1.3 \times 10^{-10} I \qquad (6)$$

The influence of ionic strength is more pronounced for $D_{1,3}$, due to the fact that $Ag(S_2O_3)_3^{5-}$ is more negatively charged and, consequently, undergoes stronger interactions in the solution.

Table 3. α and k determined by linear regression of the $\ln|j_c|$ against E plots of Fig. 9

*Solution number**	$(c_{Ag})_t$ /mol m^{-3}	$(a_{Ag})_t$ /mol m^{-3}	α	$10^6 k$ /m s^{-1}
1	1.2	0.6	0.7	67
4.1	20	2.4	0.8	5
5	40	7.0	0.7	5
11	200	8.4	0.6	3

* Solution numbers as in [1].

3.1.2. Determination of the charge transfer parameters. The charge transfer current density was calculated using Equation 1 by subtraction of the mass transfer term, modelled above, from the total current density. The variation of the logarithm of the absolute value of j_c as a function of potential is represented in Fig. 9 for four solutions of strongly different composition, and the relationship is linear. This indicates that charge transfer contributes to the total current density, as described by the proposed model. Assuming that all silver components are reduced with the same rate constant, a_b is equal to $(a_{Ag})_t$, and α can be deduced from the slope of k from the intercept of the regression equation. The results are listed in Table 3.

For α an average value of 0.7 is found, but it is difficult to decide whether it is constant or not. k is clearly a function of the solution composition.

To explain this result, different mechanisms, including chemical reaction steps, can be considered and the corresponding rate equations can be formulated [7–12]. In [13] a number of these are elaborated in detail, but only two give the required dependence of potential and solution composition:

(i) a CE mechanism in which one of the silver compounds is reduced (E) much faster than the others. They associate or dissociate (C) to form the species which can be reduced. The rate equation (in the presence of an excess ligand, which is the case for all experiments) is then

$$j_c = -Fk_0\beta_{\ln} a^n_{S_2O_3^{2-}} a_{Ag^+} \exp\left(\frac{-\alpha FE}{RT}\right) \qquad (7)$$

with $n = 1$, 2 or 3.

(ii) a parallel mechanism, in which all silver components, in equilibrium with each other, are reduced.

Table 4. Line shape parameters of the Ag peaks of standard samples

Sample	H_1/H_2	*Width /eV*
Polycyrstalline Ag	9.3 ± 0.4	8 ± 1
Evaporated Ag	10.0 ± 1	8 ± 1
Ag_2S	10.5 ± 2	8 ± 1
Ag_2O	7.0 ± 1	11 ± 1
Ag_2SO_4	4.9 ± 1.5	11 ± 1

$H_1/H_2 = I_{M_{4,5}VV}/I_{M_{4,5}N_{2,3}V}$ = amplitude ratio of the $M_{4,5}VV$ and $M_{4,5}N_{2,3}V$ peaks;
Width = energy difference between maximum and minimum of the peak.

Assuming equal transfer coefficients for all reduced species this results in the rate equation

$$j_c = -F(k_{0,0} + \sum_{i=1}^{1} \beta_{1i} a^i_{S_2O_3^{2-}} k_{i,0}) a_{Ag^+} \exp\left(\frac{-\alpha FE}{RT}\right) \quad (8)$$

with 1 = 1, 2 or 3.

Equations 7 and 8 can be rewritten as

$$j_c = -Fk a_{Ag^+} \exp\left(\frac{-\alpha FE}{RT}\right) \quad (9)$$

with

(i) for the CE mechanism

$$k = k_0 \beta_{1n} a^n_{S_2O_3^{2-}} \qquad n = 1, 2 \text{ or } 3 \quad (9a)$$

(ii) for the parallel mechanism

$$k = k_{0,0} + \sum_{i=1}^{1} \beta_{1i} a^i_{S_2O_3^{2-}} k_{i,0} \qquad 1 = 1, 2 \text{ or } 3 \quad (9b)$$

In order to discriminate between the two mechanisms, measurements were performed in solutions with varying thiosulphate concentrations [1].

k and α were determined from the $\ln|j_c|$ against E plots according to Equation 9. For α an average value of 0.75 was found and the hypothesis of equal transfer coefficients for all reduced species was retained. In Fig. 10, k is plotted against the activity of free thiosulphate. The correlation is linear, complying with the following regression equation:

$$k = 1.1 \times 10^5 + 1.9 \times 10^4 a_{S_2O_3^{2-}} \quad (10)$$

This indicates that Equation 9b applies with 1 = 1, which means that the reduction of silver thiosulphate complexes follows a parallel mechanism in which Ag^+ and $Ag(S_2O_3)^-$ are involved as shown in Scheme 1. The chemical reactions in Scheme 1 are in equilibrium.

$$\begin{array}{ccc} Ag(S_2O_3)^- + e & \xrightarrow{-k_1} & [Ag(S_2O_3)^-]^- \\ \beta_{11} \downarrow\uparrow & & \downarrow\uparrow \beta_{11}^- \\ Ag^+ + S_2O_3^{2-} + e^- & \xrightarrow{k_0} & Ag + S_2O_3^{2-} \end{array}$$

Scheme 1. Mechanism of the reduction of silver thiosulphate complexes

The reaction scheme predicts the formation of a deposit composed of Ag and $[Ag(S_2O_3)^-]^-$. Their ratio depends on the $S_2O_3^{2-}$ concentration, but also on the value of β_{11}^-, which cannot be deduced from the linear sweep voltammograms.

Therefore, the composition of the silver deposits is determined as a function of the $S_2O_3^{2-}$ concentration of the electrolyte by means of surface analytical techniques.

Table 5. Line shape parameters of the S peaks of standard samples

Sample	*Peak splitting (Individual peak positions of the composed peak) /eV*	H_+/H_-*
Ag_2S	weak 148 ± 1; 152 ± 1	0.63 ± 0.02
Ag_2SO_4	strong 133 ± 1; 148 ± 2; 156 ± 1	not to determine
$Na_2S_2O_3$	strong 130 ± 3; 142 ± 3; 152 ± 3	not to determine
$K_2S_2O_3$	strong 129 ± 5; 141 ± 5; 150 ± 5	not to determine

* H_+/H_- = amplitude ratio of positive (+) and negative (−) excursion of the main peak = asymmetry of the LVV peak with respect to the base line.

Table 6. Line shape parameters of the O peaks of standard samples

Sample	H_1/H_2*	H_+/H_-†
Ag_2O	2.8 ± 0.2	0.88 ± 0.04
Ag_2SO_4	3.4 ± 0.4	0.83 ± 0.1
$Na_2S_2O_3$	3.9 ± 0.2	0.69 ± 0.1
$K_2S_2O_3$	3.7 ± 0.4	0.73 ± 0.1

* $H_1/H_2 = I_{KVV}/I_{KL_1V}$ = amplitude ratio of the KVV and KL_1V peaks
† H_+/H_- = amplitude ratio of positive (+) and negative (−) excursion of the KVV peak = asymmetry of the KVV peak with respect to the base line.

3.2. *Surface analysis*

The analysis was mainly done using AES. The Auger analysis gives a wide variety of information about the surface layer of the specimen of about 1 nm thickness: not only component identification [14–16], but also chemical state identification [17–24] and structural information [25]. Chemical state identification is based on the line shape analysis of Auger peaks and requires comparison of the spectra of the unknown sample with spectra of standard samples of known composition.

The characterization of the silver deposits proceeds in three steps: (a) analysis of the spectra of a number of standard Ag, S and O samples of known composition; (b) selection of the line shape parameters for chemical and structural state identification for the

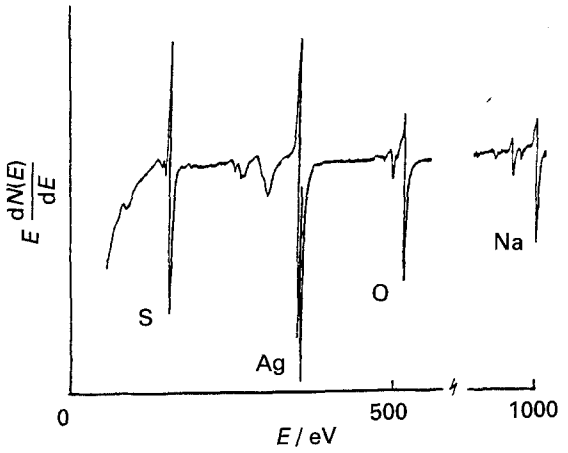

Fig. 11. Auger spectrum of the silver deposit.

three elements; and (c) analysis of the silver deposits by comparison of their spectra and line shape parameters with those of the standards.

3.2.1. Standard samples. The following standard samples were selected: polycrystalline and evaporated Ag, Ag_2S, Ag_2O, Ag_2SO_4, $Na_2S_2O_3$ and $K_2S_2O_3$. $Ag_2S_2O_3$ was not available.

Spectra were taken and line shape analysis was performed on the Ag, S and O peaks. For each of the elements, parameters for chemical and structural information were selected. These are given in Tables 4 to 6, together with their values for the different standards.

The presence of an oxygenous anion is reflected in the line shape of the Ag and S peaks and, in addition, the asymmetry of the O peak allows a distinction between oxide, sulphate and thiosulphate to be made. Consequently, a combined line shape analysis of the Ag, S and O peaks makes it possible to diagnose the presence of a silver thiosulphate compound.

3.2.2. Silver deposits. Silver deposits were formed in solutions containing, respectively, 0.14 and 1.1 M $S_2O_3^{2-}$ at a low (corresponding to a current density in the intermediate kinetic regime) and a high (corresponding to the limiting current density) overpotential. Deposition times were chosen in such a way that all deposits had the same theoretical thickness. Each deposition was performed twice in a fresh solution, and each deposit was analysed on three different spots on the surface.

Table 7. Line shape parameters of the S, Ag and O peaks of the silver deposits (line shape parameters as defined in Tables 4 to 6)

Peak	*Line shape parameter*	*Result*
S	Peak splitting	none
	asymmetry H^+/H^-	0.75 ± 0.06
Ag	Width	8.7 ± 0.2 eV
	amplitude ratio H_1/H_2	11.0 ± 0.5
O	Amplitude ratio H_1/H_2	6 ± 1
	asymmetry H^+/H^-	0.35 ± 0.10

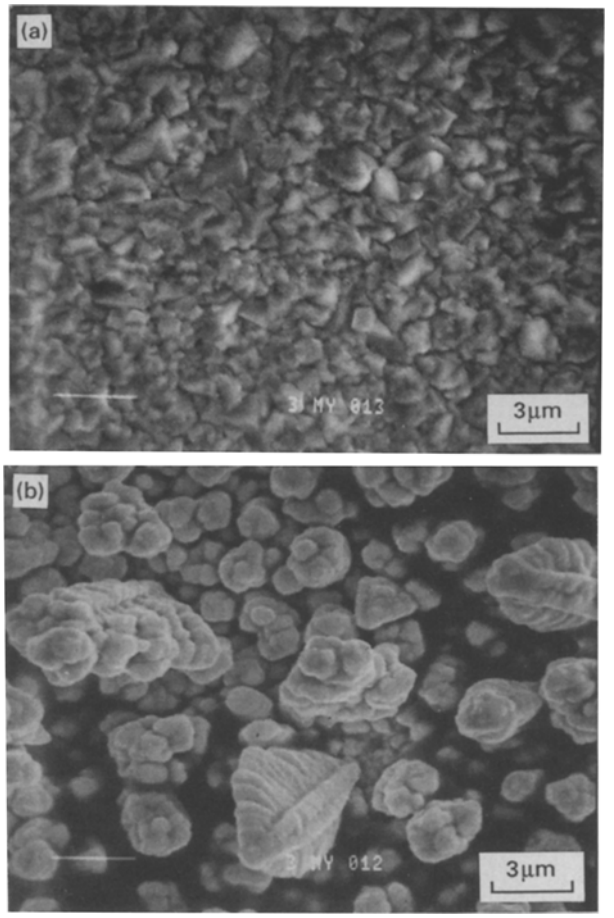

Fig. 12. SEM pictures of silver deposit at (a) low current density and (b) limiting current density.

Analogue spectra were found for the four types of deposit. A typical example is given in Fig. 11, showing the presence of S, Ag, O and Na. O and Na are not present all over the surface, but are always found together. S is detected everywhere but the intensity of its peak, relative to the intensity of the Ag peak, varies. For the S, Ag and O peaks, line shape analysis was performed according to the parameters of Table 4 to 6. The results are given in Table 7. The reported values are the average of 24 determinations (two times three for each of the four deposits).

Comparison of the values of the line shape parameters of the silver deposit with the standard sample values shows that neither Ag or S are bonded to an oxygenous anion. The presence of Ag_2S can be rejected, based on the line shape parameters of S and the varying intensity ratio of the Ag and S peaks. In accordance with the results of [26], S is thought to be present as an S^0 adsorption layer. The line shape parameters of the O peak being completely different from those of the standard samples, together with the fact that its appearance is linked with that of sodium, suggests the presence of remnants of the supporting electrolyte, $NaNO_3$, on the surface.

For deposits formed at low current density, depth profiles indicate S, O and Na only to be present in the outer surface layers. The bulk of the deposit is composed of silver, and is polycrystalline, since the diffractograms correspond completely to those of

pure polycrystalline silver [13, 27]. Consequently, the value of β_{11}^-, the equilibrium constant of the chemical reaction

$$[Ag(S_2O_3)^-]^- \leftrightarrow Ag + S_2O_3^{2-}$$

is very small. This is due to the fact that $[Ag(S_2O_3)^-]^-$ is large compared to silver, and much more difficult to incorporate in the crystal lattice of the deposit.

For deposits formed at the limiting current density, S and O were still detected after a long total sputtering time compared to that for the low current density deposits. Figure 12 shows SEM pictures of the two types of deposits: a fine and flat structure at low current density compared to the dendritic structure at the limiting current density. Due to its roughness, the depth profile of the dendritic deposit is very broad and, even after a long total sputtering time, surface components are detected.

4. Conclusion

Using a combination of electrochemical and surface analytical techniques, the mechanism of the reduction of silver thiosulphate complexes has been determined.

The reduction rate is controlled by mass transfer and the electrode reaction. Free silver ions and different complexes are present in the solution in equilibrium with each other. Mass transfer to the electrode is determined by diffusion of $Ag(S_2O_3)_2^{3-}$ and $Ag(S_2O_3)_3^{5-}$, each with its own distinct diffusion coefficient.

At the electrode, Ag^+ and $Ag(S_2O_3)^-$ are reduced at different rates, with a ratio inversely proportional to the $S_2O_3^{2-}$ concentration, respectively to Ag and $[Ag(S_2O_3)^-]^-$, in equilibrium with each other.

The deposits are composed of polycrystalline silver, indicating that the complexes decompose before or after the charge transfer reaction.

The kinetics comply with the following rate equation:

$$1/j = 1/j_c + 1/j_m$$

$$j_c = -F(k_{0,0} + k_{1,0}\beta_{11}a_{S_2O_3^{2-}}\exp\left(\frac{-\alpha FE}{RT}\right)a_{Ag^+}$$

$$j_m = -F\,0.62\nu^{-1/6}\omega^{1/2}(D_{1,2}^{2/3}c_{1,2} + D_{1,3}^{2,3}c_{1,3})$$

with

$$k_{0,0} = 1.1 \times 10^5\,m\,s^{-1}$$

$$k_{1,0} = 2.9 \times 10^{-2}\,m\,s^{-1}$$

$$\alpha = 0.75$$

$$\beta_{11} = 6.6 \times 10^5\,mol^{-1}\,m^3$$

$$D_{1,2} = 6.8 \times 10^{-10} - 6.4 \times 10^{-11} I\,m^2\,s^{-1} (I \text{ in M})$$

$$D_{1,3} = 7.2 \times 10^{-10} - 1.3 \times 10^{-10} I\,m^2\,s^{-1} (I \text{ in M})$$

$$T = 298\,K$$

From an electrochemical point of view, thiosulphate baths offer a promising alternative to toxic cyanide plating baths. Both for electrodeposition and photographic application, knowledge of the mechanism and kinetics of the reduction of silver thiosulphate complexes is the foundation for systematic study of the influence of bath composition and operating conditions on the properties of silver deposits.

References

[1] A. Hubin and J. Vereecken, *J. Appl. Electrochem.* **24**(3) (1994) 239.
[2] B. Van der Linden, H. Terryn and J. Vereecken, *ibid.* **20** (1990) 798.
[3] V.G. Levich, 'Physicochemical Hydrodynamics', Prentice-Hall, Englewood Cliffs, NJ (1962).
[4] C.M.A. Brett, *Portugaliae Electrochimica Acta* **3** (1985) 259.
[5] J.S. Newman, 'Electrochemical Systems', Prentice-Hall, Englewood Cliffs, NJ (1973).
[6] R.A. Robinson and R.H. Stokes, 'Electrolyte Solutions', 2nd edn, Butterworths, London (1959).
[7] K.J. Vetter, 'Electrochemical Kinetics. Theoretical and Experimental Aspects', Academic Press, New York (1967).
[8] C.H. Bamford and R.G. Compton, 'Comprehensive Chemical Kinetics', Vol. 26, Elsevier Science (1986).
[9] W. Vielstich and H. Gerischer, *Z. Phys. Chem.*, N.F., **4** (1955) 10.
[10] H. Gerischer, *Z. Elektrochemie* **64**(1), (1960) 29.
[11] C.P.M. Bongenaar, A.G. Remijnse, M. Sluyters-Rehbach and J.H. Sluyters, 'Network analysis of the dropping mercury electrode impedance. A mechanistic study of the Cd (II) reduction in some halide solutions' Proefschrift aan de Rijksuniversiteit Utrecht, Nederland (1980).
[12] L. Kisova, M. Sluyters-Rehbach and J.H. Sluyters, *J. Electroanal. Chem.* **40** (1972) 29.
[13] A. Hubin, 'Bijdrage tot de studie van de elektrochemische reductie van zilverthiosulfaat- en zilverthiocyanaat complexen', PhD, Vrije Universiteit Brussel, Fac.T.W. (1989).
[14] D. Briggs and M.P. Seah, 'Practical Surface Analysis by Auger and X-ray Photoelectron Spectroscopy', John Wiley & Sons, New York (1983).
[15] M. Thompson, M.D. Baker, A. Christie and J.F. Tyson, 'Auger Electron Spectroscopy', John Wiley & Sons, New York (1985).
[16] M.F. Chung and L.H. Jenkins, *Surf. Sci.* **22** (1970) 479.
[17] H.H. Madden, *J. Vac. Sci. Technol.* **18**(3), (1981) 677.
[18] B. Carrière, J.P. Deville and P. Humbert, *J. Microsc. Spectrosc. Electron,* **10** (1985) 29.
[19] D.T. Quinto and W.D. Robertson, *Surf. Sci.* **27** (1971) 645.
[20] D. Chattarji, 'The Theory of Auger Transitions', Academic Press, New York (1976).
[21] C.N.R. Rao, D.D. Sarma and M.S. Hegde, *Proc. R. Soc. Lond.* **A370** (1980) 269.
[22] R. Weissmann, *Solid State Commun.* **31** (1979) 347.
[23] S. Yashonath and M.S. Hegde, *Proc. Indian Acad. Sci. (Chem. Sci.)* **89**(5), (1980) 489.
[24] A. Hubin, H. Terryn, J. Vereecken, M. Moens and F. Adams, *Surf. Interface Anal.* **9** (1986) 327.
[25] H. Terryn, A. Laudet and J. Vereecken, *Proc. Fifth Int. Conf. Quantitative Surface Analysis,* (1988).
[26] M.M. Perdereau, *C.R. Acad. Sc. Paris* **274** (1972) 448.
[27] Joint Committee on Powder Diffraction Standards (1974).